Mathematical Biosciences and Engineering

https://www.aimspress.com/journal/mbe

MBE, 23(5): 1251–1268.
DOI: 10.3934/mbe.2026045
Received: 19 January 2026
Revised: 21 February 2026
Accepted: 10 March 2026
Published: 31 March 2026

Research article

Cost-effectiveness and optimal control analysis of an $SIR-P$ model for rodent-transmitted infection in agricultural environments

Mahmoud Moustafa*

Department of Computer Science, College of Engineering and Information Technology, Onaizah Colleges, Qassim 56447, Saudi Arabia

* **Correspondence:** Email: m.mahmoud@oc.edu.sa, mahmoudmoustafa949@gmail.com.

Abstract: Rodent populations in agricultural environments serve as critical reservoirs for zoonotic diseases, posing significant risks to food security and public health. Transmission in these settings is complex, thereby occurring through both direct rodent-to-rodent contacts and indirect exposures to environmental contamination. In this paper, we formulate and analyze a deterministic model that integrates rodent population dynamics with an environmental pathogen compartment. To identify resource-efficient mitigation policies, we develop an optimal control framework that incorporates three time-dependent interventions: contact prevention, environmental sanitation, and treatment. By applying Pontryagin's Maximum Principle, we derive the Hamiltonian, the adjoint system, and the characterization of the optimal controls, and subsequently solve the optimality system using a forward-backward sweep algorithm. We evaluate the epidemiological impact and economic viability of seven distinct intervention strategies using the Average Cost-Effectiveness Ratio (ACER) and the Incremental Cost-Effectiveness Ratio (ICER). Numerical simulations demonstrate that while the full combination of controls yields the maximum reduction in infection, the prevention-only strategy emerges as the most economically attractive option under restricted budgets. These findings suggest that prioritizing contact-reduction measures provides the most cost-effective basis for disease management, while integrated sanitation and treatments should be scaled based on resource availability. This study provides a quantitative framework that may assist agricultural stakeholders in developing resource-efficient control policies.

Keywords: mathematical modelling; $SIR-P$ model; optimal control; cost-effectiveness analysis; rodent control

1. Introduction

Rodents are among the most pervasive vertebrate pests in agricultural landscapes and are responsible for substantial economic losses through crop destruction, the contamination of stored products, and the transmission of zoonotic infectious agents. In farming communities, infestations compromise both field production and post-harvest systems, where contaminated grain and feed reduce the quality and increase the health risks for humans and livestock. Many rodent-borne infections persist in wild and peridomestic settings and are sustained by a combination of direct host-to-host contacts and indirect exposures to contaminated environments [1–3].

Mathematical modeling provides a principled framework to understand these transmission mechanisms and to evaluate intervention strategies by linking the host's demography, pathogen persistence, and environmental drivers [4]. Unlike settings where demographic processes can be neglected over short outbreak horizons, rodent birth and death may occur on a timescale comparable to the infection dynamics; consequently, management actions can alter both the population density and the infection prevalence. Moreover, ecological feedbacks may yield unintended outcomes; for example, culling can sometimes increase the prevalence by reshaping contact patterns or the immune composition of the host population [5]. These considerations motivate models that explicitly integrate demography, dual transmission pathways, and pathway-targeted interventions.

A range of studies have investigated rodent-borne infections and emphasized the roles of the host's ecology and environmental forcing in shaping the transmission dynamics [1–3]. In agricultural settings, mathematical models have also examined how management actions modify the exposure risks for humans and livestock; for example, Holt et al. [6] studied leptospirosis dynamics with seasonal drivers and the effects of rodent control. More recently, Voinson et al. [7] developed a data-informed, density-dependent $SIR-P$ framework for livestock-farm environments that linked rodent demography to pathogen transmission and compared sanitation, culling, and fertility control under different pathogen life histories. In that framework, $SIR-P$ denotes a Susceptible-Infected-Recovered model augmented by an environmental pathogen compartment $P(t)$, which captures indirect transmission through pathogen accumulation and decay in the farm environment. The uncontrolled $SIR-P$ transmission structure adopted in the present work follows [7], where management actions are explored through predefined scenarios.

The present study addresses a complementary decision problem: the allocation of intervention effort over time across pathway-targeted actions when the transmission is sustained by both direct contact and an environmental reservoir, alongside the translation of these allocations into economically ranked policies under resource constraints. Therefore, we formulate a continuous-time optimal control problem with three bounded, time-dependent intervention intensities: contact prevention $u_1(t)$ acting on the direct pathway; environmental sanitation $u_2(t)$ acting on the environmental pathway; and pathogen clearance and treatment $u_3(t)$ increasing recovery. Using Pontryagin's Maximum Principle, we derive the corresponding optimality system and compute optimal trajectories via a forward-backward sweep algorithm. Then, we compare single and combined intervention packages using cost-effectiveness indicators (Average Cost-Effectiveness Ratio (ACER) / Incremental Cost-Effectiveness Ratio (ICER) with dominance screening). On the analytical side, we establish non-negativity and uniform boundedness of solutions for all $t \geq 0$, thus ensuring biological feasibility. Additionally, we derive the basic reproduction number $\mathcal{R}_0$ via the next-generation

approach and use it to characterize the local stability of the disease-free and endemic equilibria.

The explicit inclusion of the environmental pathogen compartment $P(t)$ broadens the intervention space relative to classical SIR formulations and changes the policy interpretation. Because an environmental reservoir can sustain transmission through the indirect pathway even when the infected class declines, sanitation is not merely auxiliary: it is a structural lever that simultaneously reduces indirect exposure and accelerates pathogen clearance. This structure allows us to quantify when decontamination is economically justified in addition to prevention and treatment, particularly when environmental transmission is strong or natural pathogen decay is slow [8, 9]. Related extensions of rodent-borne infection models under alternative biological assumptions can be found in [10–14].

The remainder of the paper is organized as follows; Section 2 presents the model formulation and its fundamental properties; Section 3 develops the optimal control problem and derives the necessary optimality conditions; numerical simulations and the cost-effectiveness analysis are reported in Section 4; and finally, conclusions and possible extensions are summarized in Section 5.

2. Model formulation

We consider a rodent population in an agricultural environment where infection is transmitted through two distinct pathways: direct contact between rodents and indirect exposure to pathogens shed into the environment. The total rodent population density is as follows:

$$N(t) = S(t) + I(t) + R(t),$$

where $S(t)$, $I(t)$, and $R(t)$ denote the densities of susceptible, infected, and recovered rodents, respectively. The variable $P(t)$ represents the concentration of pathogens in the environment.

Rodent recruitment is assumed to be density dependent to reflect resource limitation (food, shelter, and space) in farm environments. In particular, rodent abundance may rapidly increase under favorable conditions but typically saturates as the density rises due to competition and the finite capacity of the environment. Accordingly, we adopt a logistic-type recruitment function with carrying capacity K as follows:

$$\Lambda(N) = \left(b - \frac{rN}{K}\right)N,$$

where b is the intrinsic birth rate, and r quantifies the density dependence [15]. Natural death occurs across all rodent compartments at a constant rate d. Susceptible rodents acquire infection through direct interactions with infected rodents at a transmission rate β and through environmental exposure at a rate ρ. Infected rodents recover at a rate γ and enter the recovered class, where they are assumed to have temporary immunity. To reflect that immunity may wane in wildlife hosts (e.g., due to variable immune responses or repeated exposure), we allow the recovered rodents to lose protection and re-enter the susceptible class at a rate Θ. Consequently, the average duration of immunity is approximately $1/\Theta$ [7, 16]. Pathogens are shed into the environment by infected rodents at a rate σ and undergo natural decay at a rate τ. The resulting uncontrolled system of differential equations is given by the

following [7]:

$$\begin{aligned}\frac{dS}{dt} &= \Lambda(N) - \beta S I - \rho S P + \Theta R - dS,\\ \frac{dI}{dt} &= \beta S I + \rho S P - (\gamma + d)I,\\ \frac{dR}{dt} &= \gamma I - (\Theta + d)R,\\ \frac{dP}{dt} &= \sigma I - \tau P,\end{aligned} \tag{2.1}$$

with nonnegative initial conditions

$$S(0) \geq 0, \quad I(0) \geq 0, \quad R(0) \geq 0, \quad P(0) \geq 0.$$

2.1. Non-negativity and boundedness

Let $x(t) = (S(t), I(t), R(t), P(t))$ be a solution of (2.1) with nonnegative initial data $x(0) \in \mathbb{R}^4_+$. As shown below, the total rodent population is uniformly bounded; in particular, if $b > d$, then

$$0 \leq N(t) \leq \max\left\{N(0), \frac{K(b-d)}{r}\right\} \qquad \forall\, t \geq 0,$$

whereas if $b \leq d$, then $N(t) \leq N(0)$ for all $t \geq 0$. Consequently, $\Lambda(N(t)) = (b - \frac{r}{K}N(t))N(t) \geq 0$ for all $t \geq 0$.

To prove the positive invariance of $\mathbb{R}^4_+$, we evaluate the vector field on the coordinate hyperplanes (assuming the remaining components are nonnegative). From (2.1),

$$\dot{S}\big|_{S=0} = \Lambda(N) + \Theta R \geq 0, \quad \dot{I}\big|_{I=0} = \rho S P \geq 0, \quad \dot{R}\big|_{R=0} = \gamma I \geq 0, \quad \dot{P}\big|_{P=0} = \sigma I \geq 0.$$

Hence, $\mathbb{R}^4_+$ is positively invariant and

$$S(t) \geq 0, \quad I(t) \geq 0, \quad R(t) \geq 0, \quad P(t) \geq 0, \qquad \forall\, t \geq 0.$$

Lemma 2.1. *Let the initial conditions satisfy $S(0), I(0), R(0), P(0) \geq 0$. Then, all solutions of the $SIR{-}P$ system* (2.1) *remain uniformly bounded for all $t \geq 0$.*

Proof. Summing the first three equations of System (2.1) yields the following:

$$\frac{dN}{dt} = \Lambda(N) - dN = \left(b - \frac{rN}{K}\right)N - dN.$$

Rewriting,

$$\frac{dN}{dt} + dN = bN - \frac{r}{K}N^2.$$

Completing the square gives the following:

$$bN - \frac{r}{K}N^2 = -\frac{r}{K}\left(N - \frac{bK}{2r}\right)^2 + \frac{b^2K}{4r} \leq \frac{b^2K}{4r}.$$

Hence,

$$\frac{dN}{dt} + dN \leq \frac{b^2K}{4r}.$$

By the comparison principle,

$$\frac{dy}{dt} + dy = \frac{b^2K}{4r},$$

and we obtain

$$N(t) \leq \max\left\{N(0), \frac{b^2K}{4rd}\right\} = N_{\max}.$$

Next, consider the environmental pathogen concentration $P(t)$ as follows:

$$\frac{dP}{dt} = \sigma I - \tau P.$$

Since $I(t) \leq N(t) \leq N_{\max}$,

$$\frac{dP}{dt} + \tau P \leq \sigma N_{\max}.$$

Applying the comparison principle yields the following:

$$P(t) \leq \max\left\{P(0), \frac{\sigma N_{\max}}{\tau}\right\} = P_{\max}.$$

Therefore, all state variables remain bounded in the positively invariant region as follows:

$$\Omega = \left\{(S, I, R, P) \in \mathbb{R}^4_+ : 0 \leq N(t) \leq N_{\max},\ 0 \leq P(t) \leq P_{\max}\right\}.$$

The proof is complete.

2.2. Equilibria and stability analysis

Lemma 2.2. *Assume $b > d$. The disease-free equilibrium of the SIR–P system* (2.1) *exists and is given by $E_0 = \left(\frac{K(b-d)}{r}, 0, 0, 0\right)$. Its basic reproduction number is as follows:*

$$\mathcal{R}_0 = \frac{K(b-d)}{r(\gamma+d)}\left(\beta + \frac{\rho\sigma}{\tau}\right).$$

Proof. Following the next-generation matrix method, we isolate the infected compartments $x = (I, P)^\top$. The new infection matrix F and the transition matrix V evaluated at E_0 are as follows:

$$F = \begin{pmatrix} \beta S_0 & \rho S_0 \\ 0 & 0 \end{pmatrix}, \qquad V = \begin{pmatrix} \gamma + d & 0 \\ -\sigma & \tau \end{pmatrix}.$$

The basic reproduction number is the spectral radius of the next-generation matrix $\mathcal{K} = FV^{-1}$, which yields $\mathcal{R}_0 = \frac{S_0}{\gamma+d}\left(\beta + \frac{\rho\sigma}{\tau}\right)$. Substituting $S_0 = \frac{K(b-d)}{r}$ completes the proof.

The basic reproduction number consists of two epidemiological pathways:

$$\mathcal{R}_0 = \frac{\beta S_0}{\gamma + d} + \frac{\rho\sigma S_0}{\tau(\gamma + d)}.$$

The first term represents direct rodent-to-rodent transmission, while the second reflects indirect transmission mediated by environmental contamination (incorporating pathogen shedding, σ, environmental infectivity, ρ, and persistence, $1/\tau$).

Theorem 2.3. *Assume $b > d$. The disease-free equilibrium E_0 is locally asymptotically stable if $\mathcal{R}_0 < 1$ and unstable if $\mathcal{R}_0 > 1$.*

Proof. The Jacobian matrix at the disease-free equilibrium $E_0 = (S_0, 0, 0, 0)$ is as follows:

$$J(E_0) = \begin{pmatrix} -b & (d-b) - \beta S_0 & (d-b) + \Theta & (d-b) - \rho S_0 \\ 0 & \beta S_0 - (\gamma + d) & 0 & \rho S_0 \\ 0 & \gamma & -(\Theta + d) & 0 \\ 0 & \sigma & 0 & -\tau \end{pmatrix}.$$

The Jacobian matrix evaluated at E_0 is block triangular, and two eigenvalues are immediately

$$\lambda_1 = -b < 0, \qquad \lambda_2 = -(\Theta + d) < 0.$$

The remaining eigenvalues are those of the infected subsystem (I, P):

$$A = \begin{pmatrix} \beta S_0 - (\gamma + d) & \rho S_0 \\ \sigma & -\tau \end{pmatrix}.$$

Its trace and determinant are as follows:

$$\mathrm{tr}(A) = \beta S_0 - (\gamma + d) - \tau,$$

$$\det(A) = \tau(\gamma + d - \beta S_0) - \rho\sigma S_0, \text{respectively.}$$

Observe that

$$\det(A) > 0 \iff \gamma + d > S_0\left(\beta + \frac{\rho\sigma}{\tau}\right) \iff \mathcal{R}_0 < 1.$$

If $\mathcal{R}_0 < 1$, then $\gamma + d > \beta S_0$; hence,

$$\mathrm{tr}(A) < -\tau < 0.$$

Therefore, $\mathrm{tr}(A) < 0$ and $\det(A) > 0$, which implies that both eigenvalues of A have negative real parts. Consequently, all eigenvalues of $J(E_0)$ are negative, and E_0 is locally asymptotically stable. If $\mathcal{R}_0 > 1$, then $\det(A) < 0$, so A has one positive eigenvalue, and E_0 is unstable.

For $\mathcal{R}_0 > 1$, the $SIR-P$ system (2.1) admits a unique endemic equilibrium $E^* = (S_e, I_e, R_e, P_e)$, where

$$S_e = \frac{S_0}{\mathcal{R}_0}, \quad I_e = \frac{(d+\Theta)S_0}{\gamma + d + \Theta}\frac{(\mathcal{R}_0 - 1)}{\mathcal{R}_0}, \quad R_e = \frac{\gamma S_0}{\gamma + d + \Theta}\frac{(\mathcal{R}_0 - 1)}{\mathcal{R}_0}, \quad P_e = \frac{\sigma(d+\Theta)S_0}{\tau(\gamma + d + \Theta)}\frac{(\mathcal{R}_0 - 1)}{\mathcal{R}_0}.$$

Theorem 2.4. *Assume $b > d$ and $\mathcal{R}_0 > 1$. Then, the endemic equilibrium $E^* = (S_e, I_e, R_e, P_e)$ is locally asymptotically stable.*

Proof. The Jacobian matrix of the $SIR-P$ system (2.1) evaluated at E^* is as follows:

$$J(E^*) = \begin{pmatrix} -(b+Q) & (d-b) - \beta S_e & (d-b) + \Theta & (d-b) - \rho S_e \\ Q & \beta S_e - (\gamma + d) & 0 & \rho S_e \\ 0 & \gamma & -(\Theta + d) & 0 \\ 0 & \sigma & 0 & -\tau \end{pmatrix},$$

where $Q = \beta I_e + \rho P_e > 0$. By substituting the endemic equilibrium relations (in particular, $S_e = S_0/\mathcal{R}_0$ and $Q > 0$ for $\mathcal{R}_0 > 1$) into the characteristic polynomial

$$\chi(\lambda) = \lambda^4 + a_1\lambda^3 + a_2\lambda^2 + a_3\lambda + a_4,$$

one verifies that the Hurwitz coefficients satisfy $a_i > 0$ for $i = 1, 2, 3, 4$. Moreover, the Routh-Hurwitz determinants for a quartic,

$$\Delta_2 = a_1a_2 - a_3, \qquad \Delta_3 = a_1a_2a_3 - a_1^2a_4 - a_3^2,$$

are also positive. Therefore, all Routh-Hurwitz conditions hold, thus implying that every eigenvalue of $J(E^*)$ has a negative real part. Hence, the endemic equilibrium E^* is locally asymptotically stable.

3. Optimal control problem

To mitigate the infection spread and environmental contamination while accounting for implementation costs, we formulate an optimal control problem with three time-dependent interventions:

1). Contact prevention $u_1(t)$: reduces direct transmission by multiplying the incidence term $\beta S(t)I(t)$ by $(1 - u_1(t))$, representing measures such as rodent-proofing, limiting aggregation, or reducing contact opportunities.

2). Environmental sanitation $u_2(t)$: reduces indirect (environmental) transmission by multiplying $\rho S(t)P(t)$ by $(1 - u_2(t))$, and simultaneously increases pathogen removal by augmenting the clearance rate from τ to $\tau + \kappa_2 u_2(t)$, where $\kappa_2 > 0$ (day^{-1}) converts the dimensionless effort intensity into a rate increment. Thus, $u_2(t)$ plays a dual role: it lowers exposure and accelerates decontamination.

3). Treatment $u_3(t)$: increases recovery from γ to $\gamma + \kappa_3 u_3(t)$, where $\kappa_3 > 0$ (day^{-1}) converts the dimensionless treatment effort into a rate increment, thus representing case management and therapeutic interventions.

The controls are dimensionless intensities that satisfy $0 \le u_i(t) \le 1$ $(i = 1, 2, 3)$, where 0 denotes no effort and 1 denotes maximal effort. The admissible control set is as follows:

$$\mathcal{U} = \left\{(u_1, u_2, u_3) : [0, T] \to [0, 1]^3 \text{ measurable}\right\}. \tag{3.1}$$

This formulation preserves the dimensional consistency and retains the pathway-specific interpretation of each intervention. The controlled dynamics are as follows:

$$\begin{aligned}
\frac{dS}{dt} &= \Lambda(N) - (1 - u_1)\beta S I - (1 - u_2)\rho S P + \Theta R - dS,\\
\frac{dI}{dt} &= (1 - u_1)\beta S I + (1 - u_2)\rho S P - (\gamma + \kappa_3 u_3)I - dI,\\
\frac{dR}{dt} &= (\gamma + \kappa_3 u_3)I - \Theta R - dR,\\
\frac{dP}{dt} &= \sigma I - (\tau + \kappa_2 u_2)P.
\end{aligned} \tag{3.2}$$

The objective is to minimize the infection burden and environmental contamination while accounting for the implementation costs. We adopt a weighted-sum functional in which $A_1 I(t)$ and $A_2 P(t)$ penalize the infection prevalence and environmental pathogen burden, respectively, and the quadratic terms $\frac{1}{2} B_i u_i^2(t)$ represent the running intervention costs. The weights $(A_1, A_2, B_1, B_2, B_3)$ are interpreted as policy parameters that reflect the management priorities and relative unit costs. Accordingly, we define the following:

$$J(u_1, u_2, u_3) = \int_0^T \left[A_1 I(t) + A_2 P(t) + \frac{1}{2} \Big(B_1 u_1^2(t) + B_2 u_2^2(t) + B_3 u_3^2(t) \Big) \right] dt. \tag{3.3}$$

The control problem is posed on a fixed horizon $[0, T]$ (prescribed campaign duration), so T is fixed and the terminal states are free. We seek $(u_1^*, u_2^*, u_3^*) \in \mathcal{U}$ such that

$$J(u_1^*, u_2^*, u_3^*) = \min_{(u_1, u_2, u_3) \in \mathcal{U}} J(u_1, u_2, u_3),$$

which is subject to the controlled system (3.2). Since $\mathcal{U}$ is nonempty, closed, convex, and bounded, the state system admits a unique solution for each admissible control, and the integrand in (3.3) is continuous in the states and convex in the controls, where the standard existence results (Filippov-Cesari) guarantee at least one optimal control triple; for example, see [17, 18].

3.1. Characterization of optimal controls

By Pontryagin's Maximum Principle, define the following Hamiltonian:

$$\begin{aligned} \mathcal{H} = {} & A_1 I + A_2 P + \frac{1}{2} \sum_{i=1}^{3} B_i u_i^2 \\ & + \lambda_1 \Big(\Lambda(N) - (1 - u_1) \beta S I - (1 - u_2) \rho S P + \Theta R - d S \Big) \\ & + \lambda_2 \Big((1 - u_1) \beta S I + (1 - u_2) \rho S P - (\gamma + \kappa_3 u_3) I - d I \Big) \\ & + \lambda_3 \Big((\gamma + \kappa_3 u_3) I - (\Theta + d) R \Big) \\ & + \lambda_4 \Big(\sigma I - (\tau + \kappa_2 u_2) P \Big), \end{aligned} \tag{3.4}$$

where $\lambda_i(t)$ $(i = 1, \ldots, 4)$ are the adjoint variables associated with the state $x(t) = (S(t), I(t), R(t), P(t))$. For $\Lambda(N) = \left(b - \frac{rN}{K} \right) N = bN - \frac{r}{K} N^2$, we have the following:

$$\Lambda'(N) = \frac{d\Lambda}{dN} = b - \frac{2rN}{K}.$$

The adjoint system satisfies $\dot{\lambda}_i(t) = -\frac{\partial \mathcal{H}}{\partial x_i}$, thus yielding the following:

$$\begin{aligned} \dot{\lambda}_1(t) &= -\Big[\lambda_1(t)(\Lambda'(N(t)) - d) + (\lambda_2(t) - \lambda_1(t))((1 - u_1(t))\beta I(t) + (1 - u_2(t))\rho P(t)) \Big], \\ \dot{\lambda}_2(t) &= -\Big[A_1 + \lambda_1(t)\Lambda'(N(t)) + (\lambda_2(t) - \lambda_1(t))(1 - u_1(t))\beta S(t) + \lambda_2(t)(- (\gamma + \kappa_3 u_3(t)) - d) \\ &\quad + \lambda_3(t)(\gamma + \kappa_3 u_3(t)) + \lambda_4(t)\sigma \Big], \\ \dot{\lambda}_3(t) &= -\Big[\lambda_1(t)(\Lambda'(N(t)) + \Theta) - \lambda_3(t)(\Theta + d) \Big], \\ \dot{\lambda}_4(t) &= -\Big[A_2 + (\lambda_2(t) - \lambda_1(t))(1 - u_2(t))\rho S(t) - \lambda_4(t)(\tau + \kappa_2 u_2(t)) \Big]. \end{aligned} \tag{3.5}$$

Since the terminal time T is fixed and the terminal state is free, the transversality conditions are as follows:

$$\lambda_1(T) = \lambda_2(T) = \lambda_3(T) = \lambda_4(T) = 0. \tag{3.6}$$

The adjoint variables $\lambda_i(t)$ can be interpreted as shadow prices (marginal values): along an optimal trajectory, they quantify the first-order sensitivity of the optimal cost-to-go with respect to perturbations in the state variables (S, I, R, P) at time t. In particular, $\lambda_2(t) - \lambda_1(t)$ measures the marginal value of reducing new infections (the $S \to I$ flow), and $\lambda_4(t)$ quantifies the marginal cost of the environmental pathogen load.

The optimal controls are obtained by minimizing $\mathcal{H}$ pointwise in u_i and projecting onto $[0, 1]$ as follows:

$$u_1^*(t) = \min\left\{1, \max\left(0, \frac{\beta S(t) I(t)(\lambda_2(t) - \lambda_1(t))}{B_1}\right)\right\}, \tag{3.7a}$$

$$u_2^*(t) = \min\left\{1, \max\left(0, \frac{\rho S(t) P(t)(\lambda_2(t) - \lambda_1(t)) + \kappa_2 \lambda_4(t) P(t)}{B_2}\right)\right\}, \tag{3.7b}$$

$$u_3^*(t) = \min\left\{1, \max\left(0, \frac{\kappa_3 I(t)(\lambda_2(t) - \lambda_3(t))}{B_3}\right)\right\}. \tag{3.7c}$$

Equation (3.7b) highlights the dual role of sanitation: the term $\rho S P(\lambda_2 - \lambda_1)$ captures the incentive to reduce new infections from environmental exposure, while $\kappa_2 \lambda_4 P$ captures the incentive to accelerate pathogen removal from the environment.

4. Numerical simulations and cost-effectiveness analysis

This section presents numerical simulations to evaluate the proposed optimal control strategies for the $SIR - P$ model of rodent-transmitted infection in agricultural environments. The optimality system, consisting of the controlled state equations (3.2), the adjoint system (3.5), and the transversality conditions (3.6), is numerically solved using a forward-backward sweep method coupled with the classical fourth-order Runge-Kutta (RK4) scheme [18, 19]. We fix the simulation horizon at $T = 50$ days and discretize $[0, T]$ on the uniform grid $t_n = n\Delta t$, $n = 0, 1, \ldots, N$, with $\Delta t = 0.01$ and $N = T/\Delta t = 5000$. The effort-to-rate conversion parameters are set to $\kappa_2 = \kappa_3 = 1$ day^{-1}. The biological parameter values are adopted from Voinson et al. [7].

The terminal time T and the weights $(A_1, A_2, B_1, B_2, B_3)$ in the objective (3.3) are policy parameters. Here, T represents a time-limited management campaign, A_1 and A_2 penalize the infection burden and environmental contamination, respectively, and B_1, B_2, B_3 encode the relative unit costs of prevention, sanitation, and treatment, respectively. Since u_i are dimensionless intensities, A_1 has units of cost per infected rodent per day, A_2 has units of cost per unit of P per day, and each B_i has units of cost per day. In the baseline simulations, we use $A_1 = 0.04$, $A_2 = 10$, $B_1 = 0.01$, $B_2 = 0.34$, and $B_3 = 0.45$, which represent a regime where contamination is weighted strongly and sanitation/treatment are costlier than prevention.

The admissible controls are measurable functions that take values in $[0, 1]$ and satisfy (3.1). With quadratic running costs, the unconstrained minimizers admit interior formulas; bounds are enforced by pointwise projection, so controls may saturate at 0 or 1 when unconstrained values fall outside $[0, 1]$,

thus yielding switching-type profiles. Saturation is governed by the balance between (A_1, A_2) and B_i: larger B_i discourages high intensities, whereas larger A_1 or A_2 increases the incentive for stronger interventions. A relaxation step is used to enhance the convergence, and iterations are terminated when the discrete sup-norm change in the controls falls below a prescribed tolerance (with a maximum-iteration safeguard).

We evaluate seven intervention strategies based on the three controls: contact prevention (u_1), environmental sanitation (u_2), and treatment (u_3):

- S_1: prevention only;
- S_2: sanitation only;
- S_3: treatment only;
- S_4: prevention + sanitation;
- S_5: prevention + treatment;
- S_6: sanitation + treatment;
- S_7: full combination.

To quantify the epidemiological and economic performance of each strategy, we compute the cumulative incidence, total implementation costs, and cost-effectiveness ratios. Let $C(t)$ denote the cumulative incidence over $[0, T]$, which is defined by the following:

$$\frac{dC}{dt} = (1 - u_1(t))\beta S(t)I(t) + (1 - u_2(t))\rho S(t)P(t), \qquad C(0) = 0. \tag{4.1}$$

The total infections averted by strategy S_j are given by $T_a^{(j)} = C_0(T) - C_j(T)$, where C_0 is the baseline cumulative incidence without control. Consistent with the objective functional (3.3), the total control cost $T_c^{(j)}$ is computed as follows:

$$T_c^{(j)} = \int_0^T \frac{1}{2}\left(B_1 u_1^2(t) + B_2 u_2^2(t) + B_3 u_3^2(t)\right) dt. \tag{4.2}$$

We utilize the ACER and the ICER to rank strategies:

$$\text{ACER}^{(j)} = \frac{T_c^{(j)}}{T_a^{(j)}}, \qquad \text{ICER}(i, j) = \frac{T_c^{(i)} - T_c^{(j)}}{T_a^{(i)} - T_a^{(j)}}, \tag{4.3}$$

where strategies in the ICER calculation are ordered by increasing the effectiveness. Strategies that are more costly and less effective than an alternative are considered strictly dominated and excluded from the ICER analysis [20, 21].

4.1. Numerical results and interpretation

We evaluated the seven intervention packages S_1–S_7. Table 1 reports the total infections averted, T_a, total cost, T_c, ACER, dominance, and ICER values.

Table 1. Cost-effectiveness outcomes ordered by increasing effectiveness (T_a).

Strategy	T_a	T_c	ACER	Dominated	ICER
S_2: Sanitation only (u_2)	48.082	8.4913	0.1766	Yes	–
S_1: Prevention only (u_1)	56.662	0.2495	0.0044	No	–
S_3: Treatment only (u_3)	66.576	3.7073	0.0557	Yes	–
S_5: Prevention + Treatment (u_1+u_3)	66.896	2.5484	0.0381	Yes	–
S_6: Sanitation + Treatment (u_2+u_3)	66.910	2.4141	0.0361	Yes	–
S_4: Prevention + Sanitation (u_1+u_2)	67.099	4.4902	0.0669	Yes	–
S_7: All controls (u_1+u_2+u_3)	67.114	1.8623	0.0277	No	0.1543

4.1.1. Dynamics under single-control strategies

Figures 1–3 illustrate the impact of individually implementing prevention (u_1), sanitation (u_2), and treatment (u_3), respectively.

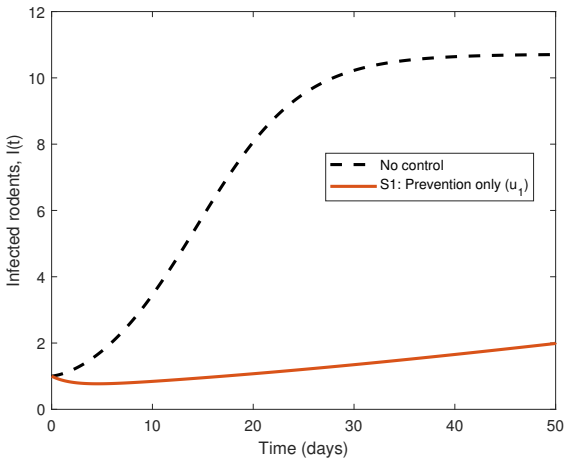

Figure 1. Dynamics of the infected rodent population $I(t)$ under strategy S_1 (contact prevention only) compared with the uncontrolled case.

Under strategy S_1 (prevention only), the infection trajectory is significantly suppressed relative to the uncontrolled case (Figure 1). While the infected population does not immediately drop to zero, it is maintained at a low level throughout the time horizon. This suggests that reducing the direct contact rate β is highly effective at stabilizing the outbreak. Economically, S_1 is the standout performer; as shown in Table 1, it averts 56.662 infections at the lowest total cost (0.2495), thus resulting in the smallest ACER (0.0044) of all strategies tested.

In contrast, strategy S_2 (sanitation only) shows the limitations of only targeting the environmental pathway (Figure 2). Although $I(t)$ is lower than the no-control scenario, it continues to grow linearly over time rather than stabilizing or declining. Furthermore, S_2 incurs the highest implementation cost (8.4913) for the lowest number of averted infections (48.082), making it a strictly dominated strategy.

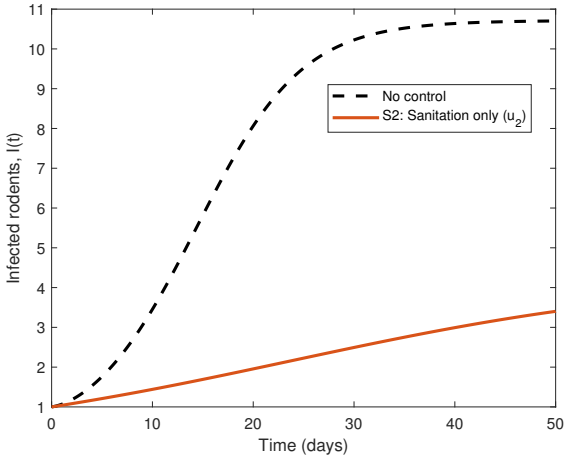

Figure 2. Dynamics of the infected rodent population $I(t)$ under strategy S_2 (sanitation only) compared with the uncontrolled case.

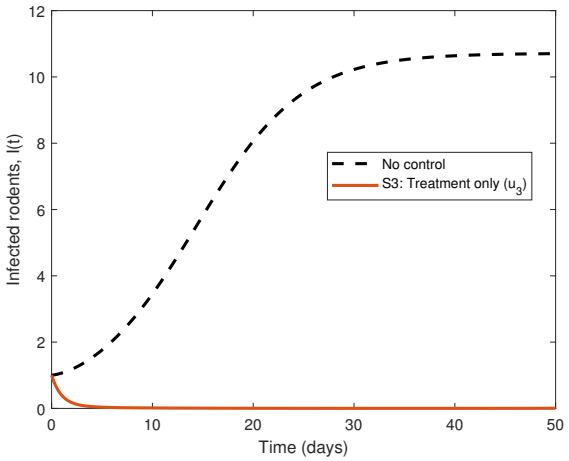

Figure 3. Dynamics of the infected rodent population $I(t)$ under strategy S_3 (treatment only) compared with the uncontrolled case.

Strategy S_3 (treatment only) demonstrates a different dynamic profile (Figure 3). By increasing the recovery rate γ, the treatment rapidly drives the infected population to near-elimination. However, this effectiveness comes at a relatively high financial cost ($T_c = 3.7073$); hence, S_3 dominated in the cost-effectiveness analysis compared to multi-control strategies that achieve similar results more cheaply.

4.1.2. Dynamics under combined strategies

Figures 4–7 depict the results of combining two or more interventions.

The simulations for the combined strategies (S_4, S_5, S_6, and S_7) all exhibit a similar qualitative behavior: a rapid exponential decline in the infected population $I(t)$, driving it to near-extinction within

the first 10 days. This demonstrates that simultaneously targeting multiple transmission and recovery pathways can produce a synergistic effect, thus accelerating infection elimination.

However, the cost-effectiveness analysis sharply distinguishes these strategies (Table 1). Strategies S_4, S_5, and S_6 are strictly dominated because they are either less effective or more costly than the full combination S_7. Strategy S_7 (all controls) achieves the highest total effectiveness ($T_a = 67.114$). After removing dominated strategies, the incremental comparison only leaves S_1 and S_7. The ICER calculation yields the following:

$$\text{ICER}(S_7, S_1) = 0.1543.$$

This implies that while S_1 is the optimal choice for limited budgets, upgrading to the full strategy S_7 costs approximately 0.1543 monetary units per additional infection averted.

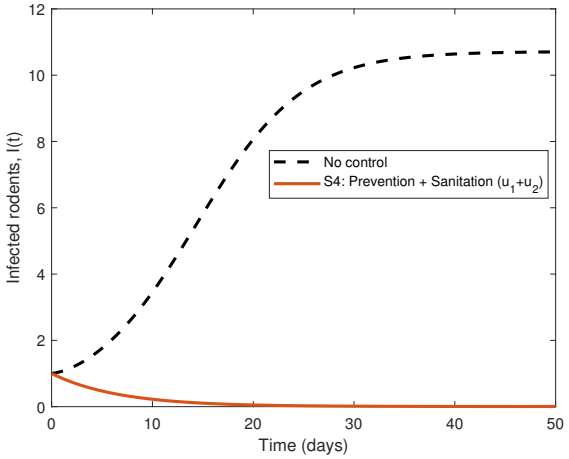

Figure 4. S_4: Prevention + Sanitation.

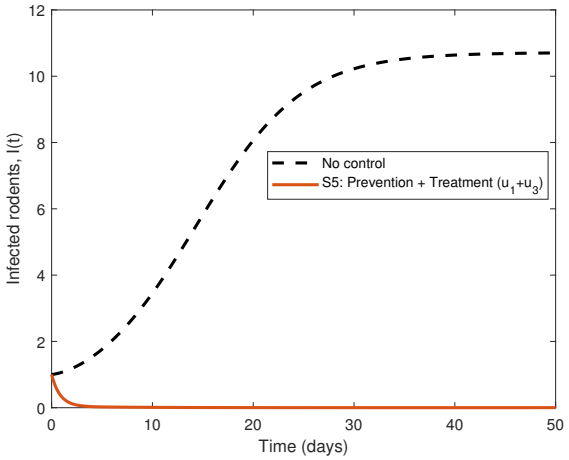

Figure 5. S_5: Prevention + Treatment.

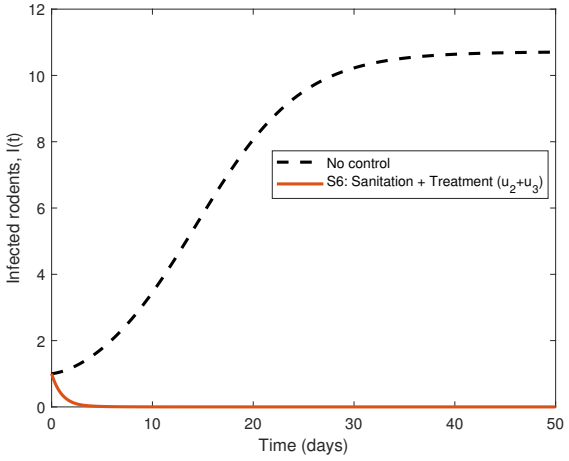

Figure 6. S_6: Sanitation + Treatment.

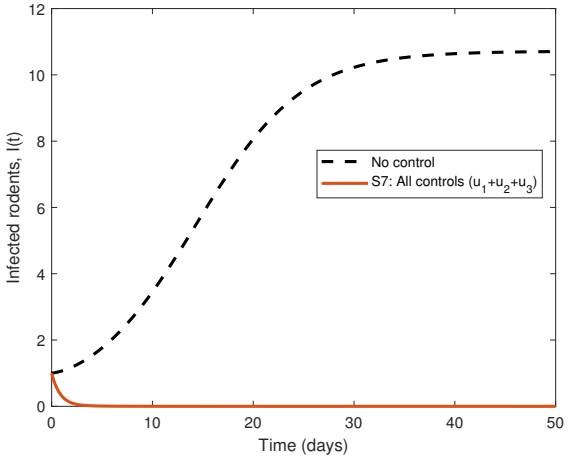

Figure 7. S_7: All controls.

In summary, the numerical results support a two-tiered policy interpretation: under strict resource constraints, contact prevention (S_1) provides the most cost-effective baseline, whereas when resources permit, the full combined strategy (S_7) yields the largest reduction in infection.

Because the ACER/ICER rankings depend on the assumed unit intervention costs, we tested the robustness with respect to (B_1, B_2, B_3) using a Monte Carlo sweep (500 draws). Each B_i was independently scaled by a log-uniform factor in $[0.5, 2]$, and for each draw, we recomputed $T_c^{(j)}$ and the resulting ACER/ICER ordering. The epidemiological effects $T_a^{(j)}$ were fixed at their baseline optimal-control values, so this is a post-optimization robustness check of the economic ranking.

Figure 8 indicates that the qualitative conclusions are stable over the explored cost regimes: S_1 remains the ACER minimizer (empirical probability 1.0), while $\{S_1, S_7\}$ consistently anchor the efficient (non-dominated) set, with S_5 only occasionally appearing (probability $\approx$ 0.14). A budget-based selection further supports a two-tier policy: under limited budgets, S_1 is preferred,

whereas for sufficiently large budgets, S_7 becomes optimal. Moreover, ICER(S_7, S_1) is stable under the cost uncertainty (median 0.1666, IQR [0.1268, 0.2022]), thus confirming that our recommendations are not driven by a single baseline cost weighting.

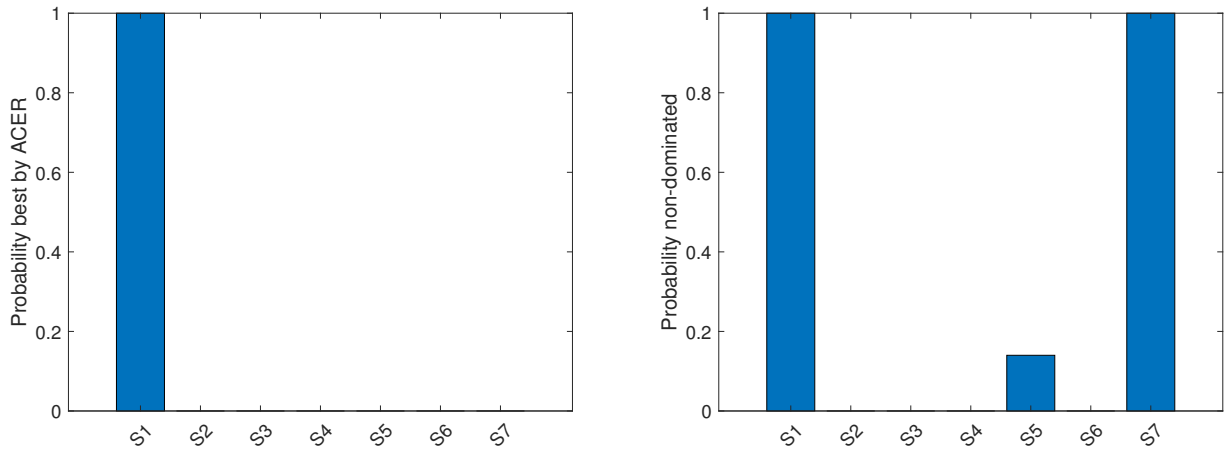

Figure 8. Monte-Carlo cost-parameter sensitivity under uncertainty in (B_1, B_2, B_3). Left: empirical probability that each strategy minimizes the ACER. Right: empirical probability of non-dominance (efficient-frontier membership).

It is instructive to contextualize these findings relative to the $SIR-P$ framework of Voinson et al. [7]. While [7] examined management options that act through rodent demography (e.g., sanitation modeled via reduced carrying capacity and culling), thereby emphasizing that the preferred option can depend on the immunity duration, the present work considers a complementary class of interventions: continuous, time-dependent controls that directly act on the transmission and recovery pathways. In particular, our formulation clarifies the mechanistic role of sanitation as a dual lever that reduces indirect exposure and increases pathogen removal through $(\tau + \kappa_2 u_2)$. When costs are explicitly accounted for via the ACER/ICER, the resulting rankings indicate that S_1 can be the most economical baseline under the assumed unit-cost regime, whereas S_7 is preferred when maximizing suppression is prioritized despite the higher marginal costs. Thus, relative to [7], our contribution is a dynamic allocation principle together with an explicit economic trade-off analysis for pathway-targeted interventions.

5. Conclusions

In this paper, we formulated and analyzed a deterministic $SIR-P$ model to investigate the transmission dynamics of rodent-transmitted infections in agricultural environments. We proved that solutions remain nonnegative and uniformly bounded for all $t \geq 0$, thus ensuring biological feasibility. We identified the disease-free equilibrium and derived the basic reproduction number $\mathcal{R}_0$ using the next-generation approach, which provides the invasion threshold. The local stability analysis showed that the disease-free equilibrium is locally asymptotically stable when $\mathcal{R}_0 < 1$ and becomes unstable when $\mathcal{R}_0 > 1$, in which case an endemic equilibrium arises.

A key feature of the model is its incorporation of dual transmission pathways, thereby accounting for both direct rodent-to-rodent contacts and indirect exposures to environmental pathogens. To identify optimal mitigation strategies, we extended this framework to an optimal control problem with three time-dependent interventions: contact prevention $u_1(t)$, environmental sanitation $u_2(t)$, and treatment $u_3(t)$. By applying Pontryagin's Maximum Principle, we derived the necessary optimality conditions, including the Hamiltonian, the adjoint system, and the explicit characterization of the optimal controls. The optimality system was numerically solved using a forward-backward sweep method coupled with a classical fourth-order Runge-Kutta scheme. We evaluated seven intervention scenarios, thus encompassing single-control and multi-control strategies, all of which reduced the infection prevalence relative to the uncontrolled baseline. To balance the biological outcomes with economic constraints, we performed a cost-effectiveness analysis based on the ACER and the ICER. Although the combined strategy (S_7) achieved the highest total effectiveness, the analysis identifies the prevention-only strategy (S_1) as the most economically efficient option, thereby yielding the lowest ACER.

The economic conclusions were not drawn from a single set of unit-cost assumptions. A Monte-Carlo sensitivity sweep over the intervention cost weights (B_1, B_2, B_3) showed that S_1 remained the ACER-minimizer across a broad range of plausible cost regimes, and that $\{S_1, S_7\}$ consistently anchored the efficient (non-dominated) set. These findings support a budget-aware interpretation: when resources are limited, contact prevention (S_1) provides a robust, economically efficient baseline; and when larger budgets are available and additional reductions are desired, upgrading toward the full package (S_7) becomes justified, with the incremental cost per additional infection averted summarized by the ICER.

Future work may consider longer horizons via terminal constraints/penalties that enforce the post-campaign suppression of $I(T)$ and $P(T)$, and by exploring maintenance-type interventions beyond T. Realism can be improved by including seasonality, spatial heterogeneity across farm microhabitats, and stochastic fluctuations in the rodent demography and pathogen persistence. Additionally, an eco-evolutionary extension could incorporate Darwinian phenotypic traits by allowing key rates (e.g., transmission, shedding, recovery, or immunity loss) to depend on heritable traits and examine how adaptation under continued intervention pressure influences persistence, stability, and long-run policy performance.

Use of AI tools declaration

The author declares he has not used Artificial Intelligence (AI) tools in the creation of this article.

Acknowledgments

The author expresses his sincere gratitude and appreciation to Onaizah Colleges, Saudi Arabia, for providing the Article Processing Charges (APC) funding for this research.

Conflict of interest

The author declares there is no conflict of interest.

References

1. T. Gedeon, C. Bodelon, A. Kuenzi, Hantavirus transmission in sylvan and peridomestic environments, *Bull. Math. Biol.*, **72** (2010), 541–564. https://doi.org/10.1007/s11538-009-9460-4
2. C. B. Jonsson, L. T. M. Figueiredo, O. Vapalahti, A global perspective on hantavirus ecology, epidemiology, and disease, *Clin. Microbiol. Rev.*, **23** (2010), 412–441. https://doi.org/10.1128/CMR.00062-09
3. G. Abramson, V. M. Kenkre, Spatio-temporal patterns in hantavirus infection, *Phys. Rev. E*, **66** (2002), 011912. https://doi.org/10.1103/PhysRevE.66.011912
4. H. W. Hethcote, The mathematics of infectious diseases, *SIAM Rev.*, **42** (2000), 599–653. https://doi.org/10.1137/S0036144500371907
5. M. Choisy, P. Rohani, Harvesting can increase severity of wildlife disease epidemics, *Proc. R. Soc. B: Biol. Sci.*, **273** (2006), 2025–2034. https://doi.org/10.1098/rspb.2006.3554
6. J. Holt, S. Davis, H. Leirs, A model of leptospirosis infection in an African rodent to determine risk to humans: Seasonal fluctuations and the impact of rodent control, *Acta Trop.*, **99** (2006), 218–225. https://doi.org/10.1016/j.actatropica.2006.08.003
7. M. Voinson, B. V. Broecke, H. Leirs, V. Sluydts, Modeling rodent population and pathogen dynamics in agricultural environments: Assessing the impact of control strategies on disease transmission, *Ecol. Modell.*, **507** (2025), 111168. https://doi.org/10.1016/j.ecolmodel.2025.111168
8. K. Mokni, M. Ch-Chaoui, Exploring persistence, stability, and bifurcations: A Darwinian Ricker–Cushing model, *Int. J. Dynam. Control*, **13** (2025), 34. https://doi.org/10.1007/s40435-024-01539-9
9. M. Ch-Chaoui, K. Mokni, A discrete evolutionary Beverton–Holt population model, *Int. J. Dynam. Control*, **11** (2023), 1060–1075. https://doi.org/10.1007/s40435-022-01035-y
10. F. M. Yusof, F. A. Abdullah, A. I. Md. Ismail, Modeling and optimal control on the spread of hantavirus infection, *Mathematics*, **7** (2019), 1192. https://doi.org/10.3390/math7121192
11. A. K. Supriatna, H. Napitupulu, M. Z. Ndii, B. Ghosh, R. Kon, A mathematical model for transmission of hantavirus among rodents and its effect on the number of infected humans, *Comput. Math. Methods Med.*, **2023** (2023), 9578283. https://doi.org/10.1155/2023/9578283
12. Y. Li, Y. Xiao, Effects of nonlinear impulsive controls and seasonality on hantavirus infection, *Math. Biosci.*, **380** (2025), 109378. https://doi.org/10.1016/j.mbs.2025.109378
13. Y. Alnafisah, M. El-Shahed, Stochastic analysis of a hantavirus infection model, *Mathematics*, **10** (2022), 3756. https://doi.org/10.3390/math10203756
14. M. Moustafa, F. A. Abdullah, S. Shafie, Z. Ismail, Dynamical behavior of a fractional-order hantavirus infection model incorporating harvesting, *Alexandria Eng. J.*, **61** (2022), 11301–11312. https://doi.org/10.1016/j.aej.2022.05.004
15. Y. Kuang, Basic properties of mathematical population models, *J. Biomath.*, **17** (2002), 129–142.
16. L. J. S. Allen, *An Introduction to Mathematical Biology*, Pearson, 2006.

17. W. H. Fleming, R. W. Rishel, *Deterministic and Stochastic Optimal Control*, Springer Science & Business Media, 1975. https://doi.org/10.1007/978-1-4612-6380-7

18. S. Lenhart, J. T. Workman, *Optimal Control Applied to Biological Models*, Chapman and Hall/CRC, 2007. https://doi.org/10.1201/9781420011418

19. E. Jung, S. Lenhart, Z. Feng, Optimal control of treatments in a two-strain tuberculosis model, *Discrete Contin. Dyn. Syst. - Ser. B*, **2** (2002), 473–482. https://doi.org/10.3934/dcdsb.2002.2.473

20. P. Rodrigues, C. J. Silva, D. F. M. Torres, Cost-effectiveness analysis of optimal control measures for tuberculosis, *Bull. Math. Biol. Z*, **76** (2014), 2627–2645. https://doi.org/10.1007/s11538-014-0028-6

21. H. W. Berhe, A. A. Gebremeskel, Z. T. Melese, M. Al-Arydah, A. A. Gebremichael, Modeling and global stability analysis of COVID-19 dynamics with optimal control and cost-effectiveness analysis, *Partial Differ. Equations Appl. Math.*, **11** (2024), 100843. https://doi.org/10.1016/j.padiff.2024.100843

AIMS Press